Eur. Phys. J. D **22**, 13–16 (2003)
DOI: 10.1140/epjd/e2002-00226-8

THE EUROPEAN PHYSICAL JOURNAL D

Measurement of X-ray production cross-sections of Ti, V, Cr, Mn, Fe, Co, Ni and Cu molecules

Ö. Söğüt[1], E. Baydaş[2], E. Büyükkasap[3], A. Küçükönder[1], and Y. Şahin[2]

[1] Kahramanmaraş Sütçü İmam University, Faculty of Art and Science, Department of Physics, 46100 Kahramanmaraş, Turkey
[2] Atatürk University, Faculty of Art and Science, Department of Physics, 25240 Erzurum, Turkey
[3] Atatürk University, K.K. Education Faculty, Department of Physics Education, 25240 Erzurum, Turkey

Received 21 March 2002 / Received in final form 9 July 2002
Published online 12 November 2002 –

Abstract. K shell X-ray production cross-sections in the Ti, V, Cr, Mn, Fe, Co, Ni, and Cu in the molecules were studied at 59.5 keV excitation energy by using a Si(Li) detector (FWHM = 155 eV at 5.96 keV). The present results are compared with other theoretical values.

PACS. 32.30.Rj X-ray spectra

1 Introduction

Precise determinations of the X-ray production cross-sections are extremely important for atomic, molecular and radiation physics. These cross-sections are broadly used, for example, in methods of non-destructive analysis of materials, basic studies of atomic process and dose calculation in medical physics. In addition, comparison of measured X-ray production cross-section with theoretical estimates provide a check on the validity of various physical parameters such as photoionisation cross-sections, X-ray production yields and emission rates.

Experimental and theoretical emission lines and X-ray production cross-sections rates have been reported by different authors [1–10]. Mittra *et al.* have stimulated their targets by charged ion projectiles [11]. Büyükkasap measured alloying effect on X-ray production yield and production cross-sections in Cr_xNi_{1-x} and Cr_xAl_{1-x} alloys [12]. The X-ray production cross-sections of bromide and iodine compounds have been measured by Küçükönder [13]. Some attempts have been made by using data on the structure of density of states in valence band of the solids. Compounds of elements in the first transitions series, which have unpaired electron in the 3*d* shell, may be considered to have a complicated valence band structure. The chemical state of 3*d* elements especially affects K_β X-ray emission probabilities, because the state of 3*d* elements is very sensitive to external influence (chemical environment) [14]. K X-rays (K_α and K_β) are depended on the physical and chemical environment of the element in the sample. In the early studies of 3*d* metal compounds [15] the influence of chemical effects has shown differences in the K_β-to-K_α X-ray intensity ratios up to nearly 10%, L shell production yields and production cross-sections [16] up to nearly 10–20%. Such chemical effect can be caused either by varying the 3*d* electron population or by mixing of *p* states from the ligand atoms with 3*d* states of the metal or both. The change in the number of 3*d* electron population of the transition metal atom in the chemical compound modifies 3*p* orbitals much stronger than 2*p* orbitals, what must be followed by substantial modification of K_β transitions and almost no modification of K_α transitions. An additional possible reason for the chemical effect is the Coster-Kronig broading of L_2 level the width [17] and we have measured chemical effect on enhancement of Coster-Kronig transitions of L_3 X-rays [18].

In this work, K X-ray production cross-sections of compounds containing Ti, V, Cr, Mn, Fe, Co, Ni, and Cu elements were measured.

2 Experimental

Experimental measurements were carried out on the K characteristic radiations of Ti, V, Cr, Mn, Fe, Co, Ni, and Cu stimulated by 59.5 keV gamma photons of a 75 mCi ^{241}Am source molecules. Powder samples were sieved by a 400 mesh and supported on a mylar film at $\approx 2-4\times10^{-3}$ g cm^{-2} thickness. The Si(Li) detector which had 155 resolution eV at 5.9 keV and system 100 card with pulse height analyser were used to count K_α and K_β photons emitted from samples. The experimental set up and K X-ray spectra of Cr are given in Figures 1 and 2, respectively. As shown in Figure 1, the lead shield was used to avoid the direct exposure of the detector to radiation from the gamma ray source. Iron lining on its inner side was used to avoid the Pb L X-rays. The aluminium lining was used to collimate K X-rays from iron. The K shell production cross-sections have been calculated using the

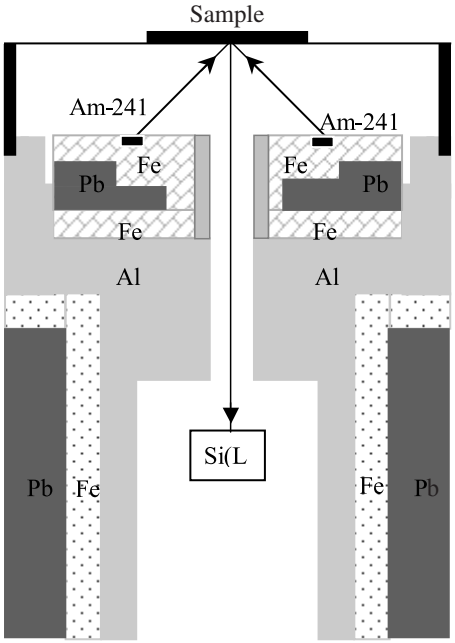

Fig. 1. Experimental set-up.

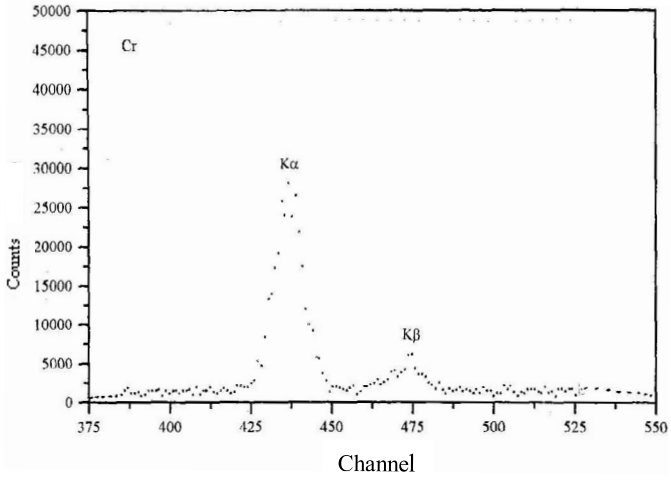

Fig. 2. Characteristic X-ray spectra of Cr.

following equation

$$\sigma_{\mathrm{K}_i} = \frac{N_{\mathrm{K}_i}}{I_0 G \varepsilon_{\mathrm{K}_i} \beta_{\mathrm{K}_i} t_{\mathrm{K}_i}} \tag{1}$$

where N_{K_i} is the intensity observed for the K_i X-ray line of the element ($i = \alpha, \beta$), I_0 is the intensity of exciting radiation, G is the geometry factor, t_{K_i} is the mass of the element in the sample ($\mathrm{g\,cm^{-2}}$), β_{K_i} is the target self-absorption correction factor for both the incident and emitted radiation, and $\varepsilon_{\mathrm{K}_i}$ is the detection efficiency of the detector at the energy of K_i X-rays. Since the self-absorption effect and detector efficiency effect are different for different energy. The corrections for these effects were made on measured values in equation (1).

$I_0 G \varepsilon$ values in the present experimental set-up were determined in a separate experiment. Target of pure elements with atomic numbers $22 \leq Z \leq 48$ emitting fluorescent X-rays in energy range 4.5–26 keV were irradiated using the same geometry and the fluorescent X-rays were counted. $I_0 G \varepsilon$ values for the present set up were therefore determined by the following equation

$$I_0 G \varepsilon_{\mathrm{K}_i} = \frac{N_{\mathrm{K}_i}}{\sigma_{\mathrm{K}_i} \beta_{\mathrm{K}_i} t_{\mathrm{K}_i}} \tag{2}$$

where σ_{K_i} is the $\sigma_{\mathrm{K}_\alpha}$ or $\sigma_{\mathrm{K}_\beta}$ production cross-sections. The self-absorption correction factor has been calculated by using the following expression obtained by assuming the incidence angle of the fluorescent X-rays subtended by detector to be approximately 90°

$$\beta_{\mathrm{K}_i} = \frac{1 - \exp\left[(-1)\left(\frac{\mu_{\mathrm{inc}}}{\cos\phi} + \mu_{\mathrm{emt}}\right) t_{\mathrm{K}_i}\right]}{\left(\frac{\mu_{\mathrm{inc}}}{\cos\phi} + \mu_{\mathrm{emt}}\right) t_{\mathrm{K}_i}} \tag{3}$$

where μ_{inc} ($\mathrm{cm^{-2}g}$) and μ_{emt} ($\mathrm{cm^{-2}g}$) are the mass absorption coefficient [19] at the incident photon energy and fluorescent X-ray energy of the sample. ϕ has been calculated by using the following expression [20]

$$\cos\varphi = \frac{\iota}{[\iota^2 + 0.25(R_0 + R_1)^2]^{1/2}} \tag{4}$$

where ι is the distance from the source to the sample, R_0 and R_1 the internal and external diameters of radioisotope source. ϕ has been calculated as 21°. In addition, we have also checked the angle, from the shift in energy of the incoherent scattered peak from the coherent peak using by Compton scattering formula.

3 Results and discussion

The obtained experimental and theoretical results are given in Table 1 as K shell production cross-sections. The errors in the experimental K-shell production cross-sections are estimated to be 6–12%. This error arises from uncertainties in the various parameters used to calculate the K production cross-sections, including errors due to peak area evaluation (<4%), $I_0 G \varepsilon$ factor (3%), target thickness measurements ($\approx$ 3%) and absorption factor ($\approx$ 2%). All errors were computed according to the classical rules of the error propagation and the resultant error is quoted on the measured production yields.

Outermost electrons participate in electron transitions from upper shell to K shell and are also emitted as Auger electrons. Auger process involves a radiationless transition. In this transition, instead of the emission of K_α and K_β lines in electronic transition from the L, M, N, ... shells to the K shell, the energy of transition is taken up to eject a second outer or outmost shell (L, M, N, ...) electron. Thus the Auger yield strongly depends on situations of outermost electrons. As seen from Table 1, even though

Table 1. K shell production cross-sections (barns/atom).

Element and compounds	Present work σ_K	Oxidation number	Symmetrical structure	Theoretical[21] σ_K
Ti	37.9±3.4	0		41.4
TiO_2	17.1±1.7	4		
V	45.8±3.9	0		48.7
VO	23.4±2.3	2		
V_2O_3	25.9±2.9	3		
V_2O_4	23.6±2.3	4		
V_2O_5	21.9±2.6	5		
Cr	54.7±4.4	0		58.4
$Cr_3(OH)_2(CH_3COO)_7$	36.3±3.5	3		
$Cr(NO_3)_3x9H_2O$	35.2±3.9	3		
Cr_2O_3	34.5±3.3	3	T_d	
$Cr(NO_3)_3$	34.5±3.3	3		
$[Cr(H_2O)_4Cl_3]$ x$2H_2O$	33.2±3.10	3		
$CrCl_3$	27.8±2.8	3		
$Cr_2(SO_4)_3H_2O$	27.1±2.2	3		
$Cr_2(SO_4)_3$ $K_2SO_4x24H_2O$	22.0±2.4	3		
$Na_2Cr_2O_7$	21.7±2.2	6	T_d	
Mn	66.1±5.2	0		70.9
MnO_2	36.8±3.7	2	O_h	
$MnSO_4$ xH_2O	34.4±3.4	2		
$Mn(CH_3COO)_3$	33.4±3.7	3		
$KMnO_4$	34.0±3.2	7	T_d	
Fe	82.3±6.8	0		83.7
FeF_3	44.9±4.5	3		
$Fe(NO_3)_3$ x$9H_2O$	43.7±3.9	3		
Fe_2O_3	39.7±2.10	3	O_h	
$FeCl_32(NH_4Cl)xH_2O$	38.9±3.2	3		
$FeNH_4(SO_4)_2x12H_2O$	38.9±3.6	3		
$FeNH_4(SO_4)_2x6H_2O$	37.0±3.3	3		
$FePO_4$	36.5±3.1	4		
Co	91.9±6.9	0		97.7
CoO	53.3±4.4	2	O_h	
CoF_2	41.9±3.4	2	O_h	
CoF_3	42.3±3.0	3		
Ni	106.7±7.7	0		113.6
$NiSO_4$	57.8±5.3	2		
$NiCl_2$	46.8±3.5	2	T_h	
Cu	117.6±8.5	0		131.3
Cu_2O	97.5±8.6	1	O_h	
CuBr	86.5±8.0	1	T_h	
CuO	88.2±8.8	2	O_h	
$Cu(CN)_2$	72.8±5.8	2		
CuC_2O_4	72.7±6.9	6		

there is not any systematic relation between K shell X-ray production cross-sections and the formal oxidation number of the element in the compound, there is a decrease in the K shell X-ray production cross-section as the oxidation number increases. The reason for this decrease may be due to the molecular structure of the samples. The molecules have different bond energies and different interatomic bond distances between ligands and central atom. Different interatomic bond distances cause different interaction between ligands and central atoms. These effects play an important role in K X-ray emission. An increase in K X-ray cross-sections is observed with increasing interatomic distances. Chemical bonding type (ionic, metallic, covalent) affects the K X-ray production cross-sections. The individual characteristics of the structure of molecules, complexes and crystals (polarity, valancy and electronegativity of atoms, coordination number, ionicities of covalent bond etc.) mainly affect the K X-ray production cross-sections. A change in chemical bond leads to a change in its valence electron density. The electron

density decreases or increases depend on type of bonding with adjacent atoms in a the molecule or crystal.

From Table 1, it can be seen that the present data are in agreement, within the experimental uncertainties, with the theoretical values of K shell production cross-sections calculated by Scofield [21] for the $3d$ elements. It is concluded that the experimental K shell production cross-section values measured in this work are in good agreement with the theoretical results for all $3d$ elements.

References

1. M.O. Krause, C.W. Nestor Jr, C.J. Sparks, E. Ricci, Oak Ridge National Laboratory Report, ORNL 5399 (1978), Oak Ridge National Laboratory, Oak Ridge, Tennesse, USA.
2. J.H. Hubbell, Rad. Phys. Chem. **59**, 113 (2000)
3. A.V. Shchagin, V.I. Pristupa N.A. Khizhnyak, Nucl. Instrum. Meth. Phys. Res. B **84**, 9 (1994)
4. G. Budak, A. Karabulut, L. Demir, Y. Şahin, Phys. Rev. A **60**, 2015 (1999)
5. I.A. Al-Nasr, I.J. Jabr, K.A. Al-Saleh, N.S. Saleh, Appl. Phys. A **43**, 71 (1987)
6. D.V. Rao, R. Cesareo, G.E. Gigante, X-Ray Spectrom. **22**, 406 (1993)
7. J.H. Hubbell, Phys. Med. Bio. **44**, R1 (1999)
8. R.A. Barrea, E.V. Bonzi, Rad. Phys. Chem. **59**, 347 (2000)
9. S. Puri, B. Chand, D. Mehta, M.L. Garg, N. Singh, P.H. Trehan, At. Data Nucl. Data Tab. **61**, 289 (1995)
10. T. Changhuan, An Z.L. Taihua, L. Zhengming, Nucl. Instrum. Meth. Phys. Res. B **155**, 1 (1999)
11. D. Mittra, M. Sarkar, D. Bhattacharya, P. Sen, G. Kuri, G. Lapicki, Nucl. Instrum. Meth. Phys. Res. B **124**, 453 (1997)
12. E. Büyükkasap, Acta Phys. Polon. A **93**, 701 (1998)
13. A. Küçükönder, Eur. Phys. J. D **17**, 293 (2001)
14. A. Küçükönder, Y. Şahin, E. Büyükkasap, Nuovo Cim. **15**, 1295 (1993)
15. A. Küçükönder, Y. Şahin, E. Büyükkasap, A. Kopya, J. Phys. B: At. Mol. Opt. Phys. **26**, 101 (1993)
16. Ö. Söğüt, E. Büyükkasap, A. Küçükönder, M. Ertuğrul, Appl. Spect. Rev. **32**, 167 (1997)
17. T. Mukoyama, X-ray Spectrom. **29**, 413 (2000)
18. Ö. Söğüt, E. Büyükkasap, M. Ertuğrul, A. Küçükönder, J. Quant. Spectrosc. Rad. Transfer **74**, 395 (2002)
19. J.H. Hubbell, S.M. Seltzer, Tables of X-ray mass attenuation coefficients and mass energy absorption coefficients 1 keV to 20 MeV for elements $Z = 1$ to 92 and 48 additional substances of dosimetric interest, U.S., Department of Commerce, Technology Administration, National Institute of Standards and Phys. Laboratory, NISTIR 5692, 1995
20. A. Zararsız, E. Aygün, J. Rad. Nucl. Chem. Art. **129**, 367 (1989)
21. J.H. Scofield, Theoretical photoionisation cross-sections from 1 to 1500 keV, Lawrence Livermore National Laboratory Report UCRL 51326, 1973